DC Breakdown Voltage of Synthetic Ester Liquid-Based Nanofluids

ABDERRAHMANE BEROUAL[1], **(Fellow, IEEE), USAMA KHALED**[2,3],
AND AASSEM M. ALGHAMDI[2]

[1]AMPERE Lab, CNRS UMR 5005, Ecole Centrale de Lyon, University of Lyon, 69134 Ecully, France
[2]Department of Electrical Engineering, College of Engineering, King Saud University, Riyadh 11421, Saudi Arabia
[3]Department of Electrical Engineering, Faculty of Energy Engineering, Aswan University, Sahary City 81528, Egypt

Corresponding author: Aassem M. Alghamdi (437105893@student.ksu.edu.sa)

ABSTRACT Synthetic esters are potential substitutes for mineral oil in power transformers owing to their biodegradability and excellent dielectric withstand. Furthermore, the addition of certain nanoparticles improves the cooling property of liquids. Both dielectric withstand and cooling are two fundamental characteristics for use in breathable components. Previous studies showed that AC breakdown voltage of synthetic ester could be increased by adding Fe_3O_4, Al_2O_3 and SiO_2 nanoparticles. This paper deals with the DC breakdown voltage of the same synthetic ester-based nanofluids. Nanofluid samples are characterized using the same techniques to those used for AC breakdown voltage study. This includes a particle size analyzer, scanning electron microscope and energy dispersive x-ray spectroscopy analyzer. Statistical analysis of experimental data using normal and Weibull laws and an estimate of DC breakdown voltage with probabilities of risk of 1% and 50% are performed. The experimental results evidence the existence of an optimum concentration of nanoparticles that gives the highest DC breakdown voltage, except SiO_2 nanoparticles which degrade the DC breakdown voltage of pure synthetic ester, regardless of the concentration. For the other two types of nanoparticles, the DC breakdown voltage is improved by approximately 25%, 13%, and 10%, with Al_2O_3 (13 nm), Al_2O_3 (50 nm), and Fe_3O_4 (50 nm) nanoparticles at the optimum concentration that is 0.05 g/L, respectively. It is also shown that the obtained results generally comply with the normal and Weibull distribution laws.

INDEX TERMS Nanofluids, breakdown voltage, normal distribution, Weibull distribution, power transformer, synthetic ester.

I. INTRODUCTION

Transformers are vital components of electrical networks and play a crucial role in the long-distance transport and distribution of electricity. Generally, transport using high voltage overhead lines is the most used means, except in certain cases where transport by cables is inevitable as is the case of connections in urban areas or the interconnections between offshore wind farms and the earth. The reactive power in the case of transport by cable; with solid or impregnated insulation; under AC voltage is greater than in the case of overhead lines or gas insulating lines (GIL) what reduces the power factor. This is due to the capacitance of cables; the relative permittivity (dielectric constant) of insulating (polymer or impregnated paper) in cables being higher than that of overhead lines or GIL where it is equal to 1 for air or other gas/gas mixtures. The use of high direct voltage (HVDC) enables to get rid the problem of reactive power hence the considerable interest in HVDC transport in recent years.

One critical element of a liquid-immersed power transformer is its insulating fluid, which also acts as a coolant to mitigate the risk of overheating as well as reduce electrical clearances. Until about thirty years ago, mineral oils were mostly used for this purpose. Owing to their poor biodegradability (less than 30%) and their effect on aquatic sources of mineral oils [1], new insulating liquids have been developed to replace mineral oils, and special attention has been given to ester-based fluids. Synthetic ester (SE) transformer fluids are known to have a high fire point and high moisture tolerance

---

compared with other insulating oils; they can contain up to 2000 ppm of water at 20 °C against 55 ppm for mineral oils [1]–[3]. For this reason, humidity becomes a less limiting factor for dielectric properties. Moreover, they are readily biodegradable [3]. These properties make it possible to ensure fire safety, improve the performance of transformers, and protect the environment by extending the life of the devices.

Additionally, the very low pour points and excellent oxidation stabilities make SEs usable in breathable power transformers, intended to operate in cold regions [2], [3]. These reasons explain why ester-based fluids are being increasingly used in many high-voltage applications such as medium distribution transformers, traction transformers, and now, power transformers, over the past few decades. Numerous transformers installed worldwide today are filled with ester-based fluids [3].

Despite their interesting characteristics indicated above, ester oils have several limitations, including their viscosity, which is slightly high and becomes very important at low temperatures. This characteristic is one of the harmful effects that ester oils can have on mixing with the mineral oils, especially while filling transformers.

On the other hand, the increasing demand for electric energy and, consequently, the increase in energy density increases the temperature of the windings of the transformers and poses a serious problem to the safety of the device and thus the environment. The cooling property of fluids can be further improved by adding certain types of nanoparticles (NPs) to the fluid [4]–[7]. Many investigations have shown, over the past three decades that NPs significantly improve the heat transfer of insulating liquids [4]–[10].

Some researchers have reported that in addition to exerting positive effects on the thermal transfer of insulating liquids, NPs could also considerably improve the dielectric withstand of these liquids [11]–[17].

The fact that certain NPs make it possible to improve, both heat transfer (cooling) and the dielectric strength of insulating liquids, make them potential substitutes for the base insulating oils used in oil-filled apparatus.

However, most of the results reported in literature deal with the dielectric behavior of mineral oils and esters under AC and lightning impulse voltages. To our knowledge, a very little work has been done on the dielectric strength of esters-based nanofluids under DC voltage. As indicated above, the advantage of using DC voltage makes it possible to get rid of the problem of reactive power in some specific components of electrical networks.

In previous work [18], the AC breakdown voltage (AC-BDV) of a SE, namely MIDEL 7131 in the presence of conductive (Fe_3O_4) and insulating (Al_2O_3 and SiO_2) nanoparticles (NPs) has been investigated. An improvement of the SE's AC-BDV, the level of which depends on the quantity, size, and type of NP has been observed; in addition, there is an optimal concentration at which an optimal AC-BDV (i.e., the highest value) can be obtained. The best result was obtained using conducting Fe_3O_4 (50 nm) NPs for which the AC-BDV increases by approximately 48%; an increase is of approximately 35 and 25% with Al_2O_3 for NPs of 13 and 50 nm, respectively; and an increase of approximately 32% while using SiO_2 (50 nm).

This article aims to study the influence of the same type of NPs on the DC breakdown voltage (DC-BDV) of the same SE liquid (MIDEL 7131); the goal being the comparison of breakdown voltage under DC and AC voltage waveforms in the same experimental conditions.

Statistical analysis using normal and Weibull distribution laws as well as an estimate of the DC-BDV with probabilities of risk of 1% risk and 50% are conducted.

II. EXPERIMENT
A. NANOFLUID SAMPLES PREPARATION
The investigated basic SE oil was MIDEL 7131; the main physicochemical characteristics of which have been given in previous paper [18]. Similarly, the nanoparticles NPs tested were also the same as provided in [18]: Fe_3O_4 (50 nm size), SiO_2 (10–20 nm size) and Al_2O_3 (13 and 50 nm size).

The choice of these nanoparticles is in liaison with our previous work carried out under AC [18]. The objective is to compare the dielectric strengths in DC with those already obtained in AC, for the same NFs (using the same base oil) with the same NPs and at the same concentrations.

The used methodology and experimental techniques for preparing NFs were described in previous works [18], [19]. This include the distribution of the various nanoparticles which was measured by using a particle size analyzer (NanoPlus, Particulate Systems, USA); scanning electron microscope (SEM) images; and energy dispersive x-ray spectroscopy (EDS) analysis. NFs samples were prepared by dispersing NPs in SE and submitting them to a magnetic stirring process for 30 min. The samples were then placed in the ultrasonic homogenizer for 2 h to avoid aggregation of NPs. Further ultrasonification was then applied for a 2 min duration to reach a stable suspension of nanoparticles and to avoid the use of surfactant. NFs samples were then moved into a vacuum chamber of 0.16 MPa for 24 h for drying and removal of internal micro bubbles. A Malvern Zeta sizer nano ZS 90-UK is used to check the stability of NFs.

B. TEST CELL
The used test cell is a Foster Oil Test 90 with 500 ml volume capacity and two spherical brass electrodes of 12.5 mm diameter, the electrode gap being 2.50 ± 0.05 mm, which is the same as that used in our previous work [18]. Note that prior to experimental tests, the electrodes and the test cell were cleaned with alcohol. Furthermore, the whole setup was washed using hot distilled water and then put in an oven for three hours at 50 °C. Then, the nanofluid sample was poured into the test cell, slowly, and left to rest at room temperature for 15 min to allow the removal of gas bubbles that have been introduced into the nanofluid sample during pouring.

C. EXPERIMENTAL SETUP

The breakdown voltage tests are performed using a DC high potential device (0–130 kV, 10 mA, High Voltage Inc. DC Hipot, Model PTS130F; ±1% accuracy) with negative polarity (Figure 1). A 2.5 kΩ current limiting resistor placed between the HV source and test cell enables to protect the later against excessive charging currents or over-voltages that can lead to flashover or arc discharges inside the test cell.
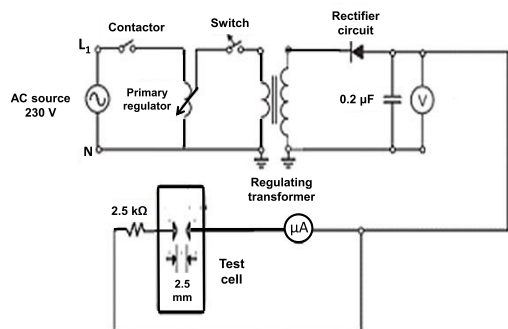

FIGURE 1. Circuit diagram of the DC test.

D. BREAKDOWN VOLTAGE MEASUREMENT AND STATISTICAL ANALYSIS METHODS

Due to the lack of standards for the measurement of DC-BDV, the same protocol as that used for measuring AC-BDV has been adopted [18]. The voltage was applied continuously with a rising rate of 2 ± 0.2 kV/s up to the point of breakdown. To stir the nanofluid samples and allow self-healing of nanofluid samples, measurements were spaced 2 minutes apart.

The statistical analysis of the DC-BDV measurements was performed using two distribution laws that are the most employed in the field of dielectric materials, namely the normal and Weibull probabilities. These two distribution laws and their application have been discussed in previous works [20], [21]. It is worth noting that this experiment pertains to answering the question as to which distribution the experimental data follows. For this, the Shapiro–Wilk test [22] and Anderson–Darling (AD) [23] test were applied. Then, by computing the *p*-value that measures the evidence against the null hypothesis [24] and by comparing it with a significance level, α, one determines whether the data complies with the normal distribution or not. Generally, $\alpha = 5\%$ is assumed as a reasonable value. For *p*-values equal to or lower than α, the null hypothesis is rejected, and hence the sample data does not belong to the considered statistical-distribution law. Note that smaller *p*-values provide stronger evidence against the null hypothesis. Larger values for the Anderson-Darling statistic indicate that the data do not follow a Weibull distribution.

III. EXPERIMENTAL RESULTS

A. AVERAGE BREAKDOWN VOLTAGE

Figures 2 to 5 illustrate the average DC-BDV of the investigated NF samples deduced from 8 measurements.

Table 1 summarizes the experimental results for the different types of NPs, their concentrations, and their sizes. The existence of an optimum value for the DC-BDV, when mixing Al_2O_3 (13 nm), Al_2O_3 (50 nm) and Fe_3O_4 (50 nm) NPs at a concentration of 0.05 g/L, was observed; the improvement in breakdown voltage was approximately 25%, 13%, and 10%, respectively. While by adding SiO_2 NPs, the DC-BDV decreases irrespective of its concentration.
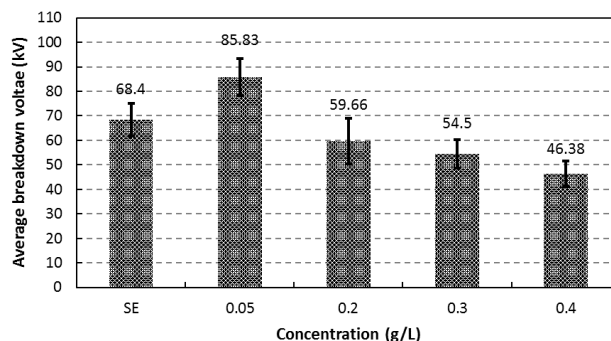

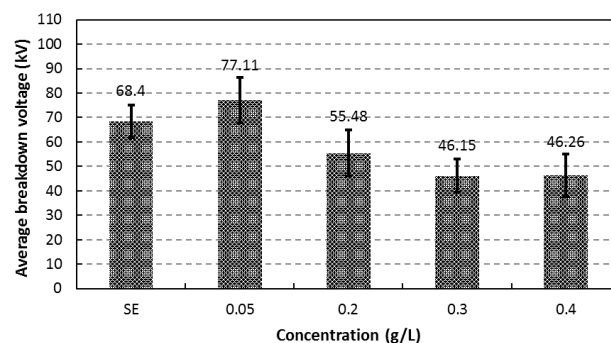**FIGURE 2. Average DC-BDV of SE/Al_2O_3 (13 nm) nanofluids.**

FIGURE 3. Average DC-BDV of SE/Al_2O_3 (50 nm) nanofluids.
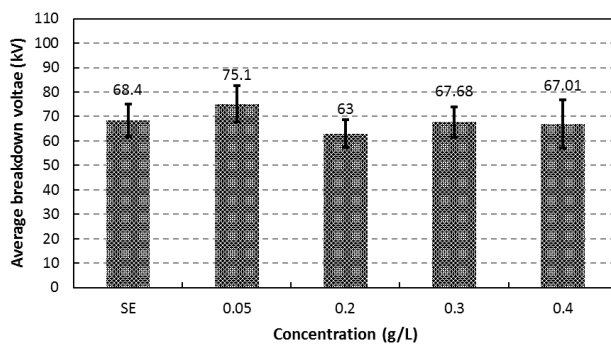

FIGURE 4. Average DC-BDV of SE/Fe_3O_4 nanofluids.

B. COMPLIANCE OF THE EXPERIMENTAL RESULTS WITH THE WEIBULL LAW

To ascertain the compliance of the experimental values with the Weibull distribution law, we used 8 successive measurements. This number being a power of two ($2^3 = 8$), it allows
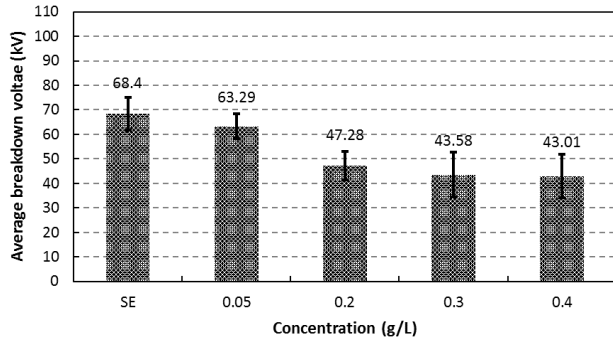
FIGURE 5. Average DC-BDV of SE/SiO$_2$ nanofluids.

TABLE 1. Average DC-BDV of the different investigated nanofluids.

	Synthetic ester oil	Fe$_3$O$_4$ (50 nm)	Al$_2$O$_3$ (50 nm)	Al$_2$O$_3$ (13 nm)	SiO$_2$ (50 nm)
		SE / 0.05 (g/L) NF			
BDV (kV)	68.40	75.10	77.11	85.83	63.29
Increment (%)		9.80	12.73	25.48	-7.47
		SE / 0.2 (g/L) NF			
BDV (kV)		63.00	55.48	59.66	47.28
Increment (%)		-7.89	-18.89	-12.78	-30.88
		SE / 0.3 (g/L) NF			
BDV (kV)		67.68	46.15	54.50	43.58
Increment (%)		-1.05	-32.53	-20.32	-36.29
		SE/ 0.4 (g/L) NF			
BDV (kV)		67.01	46.26	46.38	43.01
Increment (%)		-2.03	-32.37	-32.19	-37.12

us to deduce the slope of the Weibull plots, that is to say the shape parameter [25], [26]. Note that the breakdown voltage of NFs is not affected after 8 successive breakdown tests. We did not indeed observe any significant change in the color of samples or carbonization (contaminants) with respect to virgin nanofluid samples.

Statistical processing of experimental data, using Weibull statistics, makes it possible to determine the breakdown voltage at 63.2% cumulative probability, with a confidence interval of 95%.

Figures 6 to 10 provide the Weibull plots for the DC-BDV of SE-based Fe$_3$O$_4$, Al$_2$O$_3$, and SiO$_2$ NFs. The *p*-values, Anderson–Darling (AD), scale parameter (i.e., the scattering of experimental data), and the shape parameter are indicated for each of the figures; the shape parameter represents the slope of the line.

Table 2 gives the *p*-values and compliance of experimental results with the Weibull distribution. It is observed that for the chosen value of α ($\alpha = 5\%$), the experimental data obey the Weibull distribution law except for SE/Fe$_3$O$_4$ (0.2 g/L). In the latter case, we observe that many points are far from the line of conformity to Weibull's law.

On the other hand, it is noticed that in the particular case of SE/Fe$_3$O$_4$ NFs, the straight slopes are less steep (Figure 6)
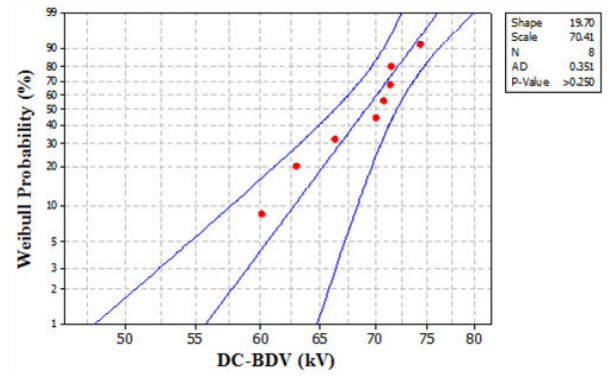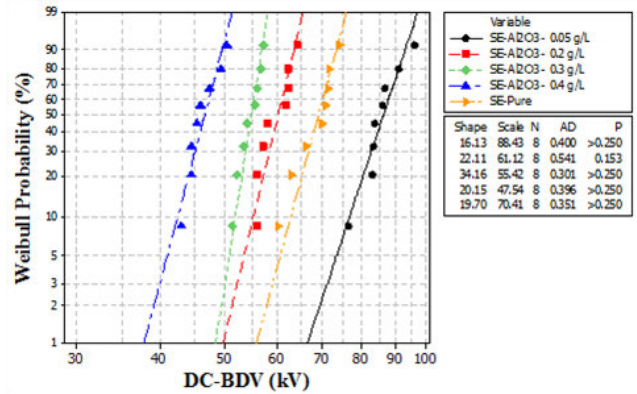

FIGURE 6. Weibull 95% probability of DC-BDV of pure SE.

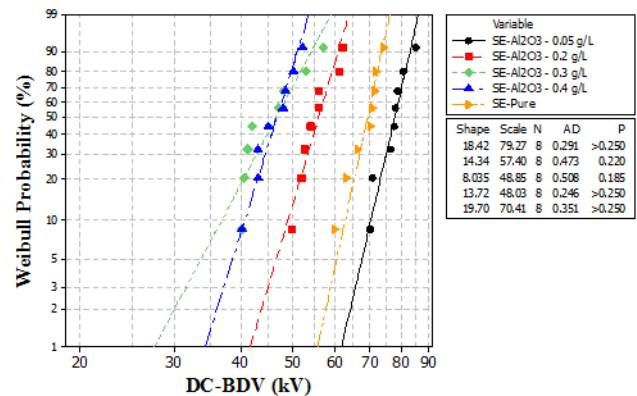**FIGURE 7.** Weibull distribution of the DC-BDV of SE/Al$_2$O$_3$ (13 nm) nanofluid.

FIGURE 8. Weibull distribution of the DC-BDV of SE/Al$_2$O$_3$ (50 nm) nanofluid.

than for the other NFs (Figures 7 to 8); this means that the dispersion of the measurement results is greater than in the other NFs. Indeed, the steeper the slope, the less the dispersion is.

The DC-BDV values at 1% and 50% cumulative probabilities are also of high interest in industrial practice. Indeed, the 1% DC-BDV represents the lowest possible DC-BDV that informs the reliability of the insulating liquid; and the 50% DC-BDV is the mean value. Table 3 summarizes the values
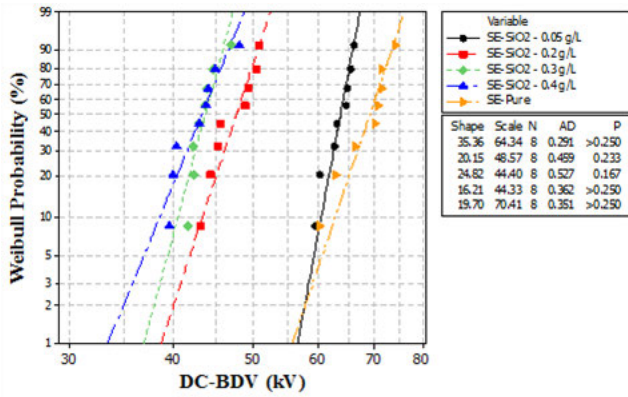
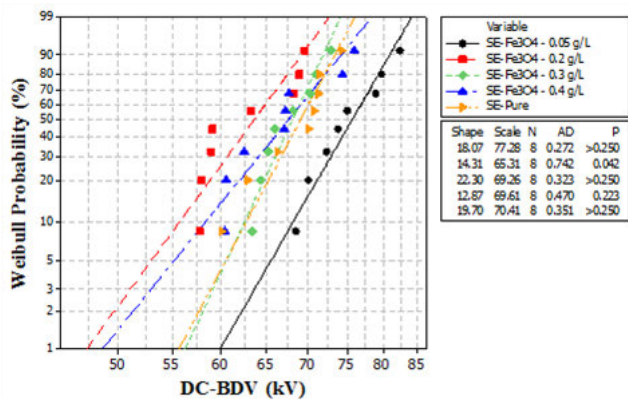**FIGURE 9.** Weibull distribution of the DC-BDV of SE/SiO$_2$ nanofluid.

FIGURE 10. Weibull distribution of the DC-BDV of SE/Fe$_3$O$_4$ nanofluid.

TABLE 2. Hypothesis test of compliance with the weibull distribution law of the average DC-BDV of nanofluids.

Sample	p-value	Conformity to Weibull distribution
Pure NE	>0.250	Accepted
SE/Fe$_3$O$_4$ (0.05 g/L)	>0.250	Accepted
SE/Fe$_3$O$_4$ (0.2 g/L)	0.042	Not Accepted
SE/Fe$_3$O$_4$ (0.3 g/L)	>0.250	Accepted
SE/Fe$_3$O$_4$ (0.4 g/L)	0.223	Accepted
SE/Al$_2$O$_3$ (13 nm) (0.05 g/L)	>0.250	Accepted
SE/Al$_2$O$_3$ (13 nm) (0.2 g/L)	0.153	Accepted
SE/Al$_2$O$_3$ (13 nm) (0.3 g/L)	>0.250	Accepted
SE/Al$_2$O$_3$ (13 nm) (0.4 g/L)	>0.250	Accepted
SE/Al$_2$O$_3$ (50 nm) (0.05 g/L)	>0.250	Accepted
SE/Al$_2$O$_3$ (50 nm) (0.2 g/L)	0.220	Accepted
SE/Al$_2$O$_3$ (50 nm) (0.3 g/L)	0.185	Accepted
SE/Al$_2$O$_3$ (50 nm) (0.4 g/L)	>0.250	Accepted
SE/ SiO$_2$ (0.05 g/L)	>0.250	Accepted
SE/ SiO$_2$ (0.2 g/L)	0.233	Accepted
SE/ SiO$_2$ (0.3 g/L)	0.167	Accepted
SE/ SiO$_2$ (0.4 g/L)	>0.250	Accepted

of the 1% and 50% breakdown probabilities. The highest 1% and 50% DC-BDV values are both obtained using Al$_2$O$_3$ (13 nm) NPs at a concentration of 0.05 g/L.

TABLE 3. Values of DC-BDV at 1% and 50% breakdown probabilities for investigating NFs deduced from weibull plots.

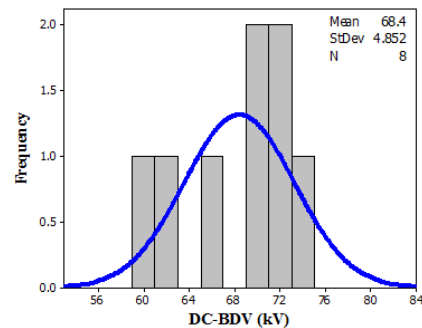| Breakdown voltage probability (%)	Breakdown voltage (kV)	Breakdown voltage (kV)	Increment (%)	Breakdown voltage (kV)	Increment (%)	Breakdown voltage (kV)	Increment (%)	Breakdown voltage (kV)	Increment (%)
	SE	0.05 g/L		0.2 g/L		0.3 g/L		0.4 g/L	
Fe$_3$O$_4$ Nanoparticles									
1	55.7	59.9	7.5	47.4	-14.9	56.4	1.3	48.7	-12.6
50	69.1	75.7	9.6	63.7	-7.8	68.1	-1.4	67.7	-2.0
Al$_2$O$_3$ (13 nm) Nanoparticles									
1	55.7	66.5	19.4	49.6	-11.0	48.4	-13.1	37.8	-32.1
50	69.1	86.4	25.0	60.1	-13.0	54.8	-20.7	46.7	-32.4
Al$_2$O$_3$ (50 nm) Nanoparticles									
1	55.7	61.8	11.0	41.7	-25.1	27.6	-50.4	34.3	-38.4
50	69.1	77.7	12.4	56.0	-19.0	46.7	-32.4	46.8	-32.3
SiO$_2$ Nanoparticles									
1	55.7	56.5	1.4	38.7	-30.5	36.9	-33.8	33.4	-40.0
50	69.1	63.7	-7.8	47.7	-31.0	43.8	-36.0	43.3	-37.3

FIGURE 11. DC histogram of DC-BDV for pure SE.

C. COMPLIANCE OF EXPERIMENTAL RESULTS WITH THE NORMAL LAW

Eight measurements were performed for this statistical analysis. The histograms for the DC-BDV distribution of the studied NF samples are depicted in Figures 11, 12, 14, 16 and 18. Thus, by computing the p-value as indicated in subsection II.C, and by comparing this value to $\alpha = 5\%$, it appears that all experimental results obey the normal distribution law. Table 4 summarizes the results of the hypothesis test of compliance with the normal distribution law for the average DC-BDV.

To verify whether the distribution frequency is normal, the skewness and kurtosis values are computed using the statistical package - *Statistical Package for the Social Sciences* (SPSS) [27]. The values of these parameters indicate the deviation from normal distribution [28]. Note that the SPSS software enables to calculate and to depict the mean, variance, skewness, kurtosis, range, standard deviation, minimum value, maximum value and probabilities U$_{1\%}$ and U$_{50\%}$ of breakdown voltage.

TABLE 4. Hypothesis test of compliance with normal distribution law of the average DC-BDV of nanofluids.

| Sample	*p*-value	Conformity to normal distribution
SE-Pure	0.256	Accepted
SE-Al$_2$O$_3$ (13 nm) - 0.05 g/L	0.542	Accepted
SE- Al$_2$O$_3$ (13 nm) - 0.2 g/L	0.136	Accepted
SE- Al$_2$O$_3$ (13 nm) - 0.3 g/L	0.546	Accepted
SE- Al$_2$O$_3$ (13 nm) - 0.4 g/L	0.570	Accepted
SE- Al$_2$O$_3$ (50 nm) - 0.05 g/L	0.513	Accepted
SE- Al$_2$O$_3$ (50 nm) - 0.2 g/L	0.441	Accepted
SE- Al$_2$O$_3$ (50 nm) - 0.3 g/L	0.193	Accepted
SE- Al$_2$O$_3$ (50 nm) - 0.4 g/L	0.774	Accepted
SE-SiO$_2$ - 0.05 g/L	0.391	Accepted
SE- SiO$_2$ - 0.2 g/L	0.298	Accepted
SE- SiO$_2$ - 0.3 g/L	0.463	Accepted
SE- SiO$_2$ - 0.4 g/L	0.502	Accepted
SE-Fe$_3$O$_4$ - 0.05 g/L	0.827	Accepted
SE- Fe$_3$O$_4$ - 0.2 g/L	0.055	Accepted
SE- Fe$_3$O$_4$ - 0.3 g/L	0.615	Accepted
SE- Fe$_3$O$_4$ - 0.4 g/L	0.329	Accepted
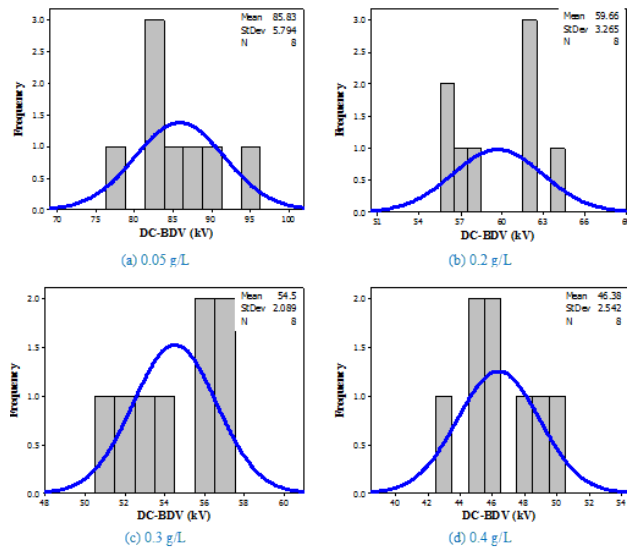
FIGURE 12. Histogram of DC-BDV for SE/Al$_2$O$_3$ (13 nm).

Figures 13, 15, 17 and 19 provide the corresponding skewness and kurtosis scores. Such representations also enable us to identify the possible anomalies in the distribution of DC-BDVs with respect to the normal distribution law.

It is noticed from the skewness coefficients that the distribution of DC-BDV is more or less asymmetrical. However, the asymmetry is rather positive indicating that the distribution of DC-BDV is asymmetric more to the left of the mean value; the accumulation scores are not on one side of distribution.

The kurtosis of investigated NFs is generally lower than 3 (the highest value is slightly higher than 2). Therefore, the distributions of BDV are platykurtic. Note that the coefficients of skewness and kurtosis of the normal distribution are respectively 0 and 3.
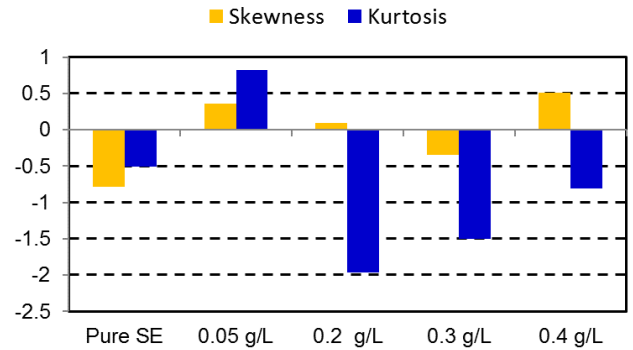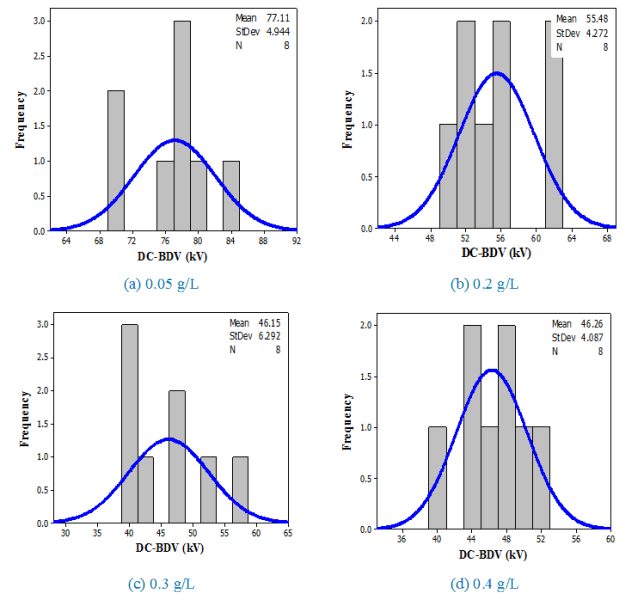
FIGURE 13. Skewness and kurtosis of DC-BDV for SE/Al$_2$O$_3$ (13 nm).

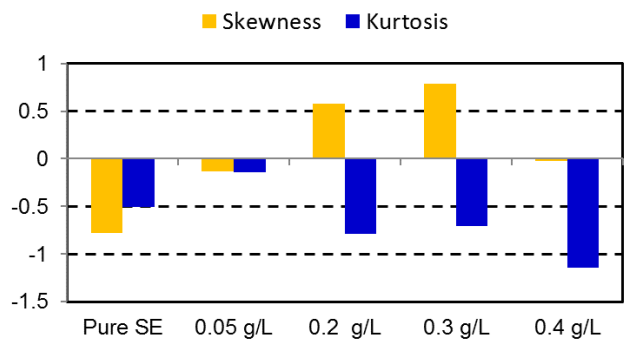**FIGURE 14.** Histogram of DC-BDV for SE/Al$_2$O$_3$ (50 nm).

FIGURE 15. Skewness and Kurtosis of DC-BDV for SE/Al$_2$O$_3$ (50 nm).

According to the *p*-value, the experimental values of DC-BDV are in accordance with the distribution of normal law whereas while being based on the skewness scores which are not zero, the experimental results do not conform to the normal distribution. This could be due to the choice of the value of α.
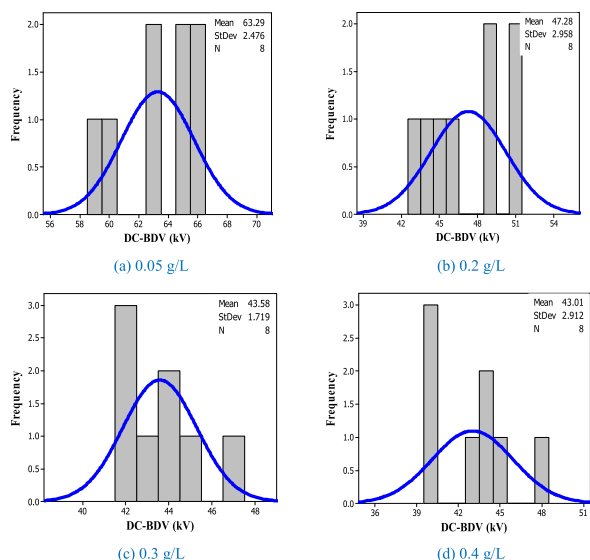
FIGURE 16. Histogram of DC SE/SiO$_2$.

FIGURE 17. Skewness and kurtosis of DC SE/SiO$_2$.

The conformity of breakdown voltage with the statistical law is used to determine the statistical probability of the breakdown voltage. That is to say a probability of $\beta(\%)=P(U\leq U_\beta)$ or $U_{\beta\%}$ whose BDV is not below the voltage U_β. The BDV at low probability also determines the safety factor of a sample in the design of electrical equipment.

Note that the values of DC-BDV at 1% and 50% of the cumulative probability deduced from the normal law distribution are identical to those deduced from the Weibull plots given in Table 3.

IV. DISCUSSION

It appears from the above results that the addition of Al$_2$O$_3$ and Fe$_3$O$_4$ nanoparticles increases the DC-BDV of the investigated SE; and at an optimum concentration of 0.05 g/L these NPs for which the DC-BDV is the highest, exists. The optimum value of the DC-BDV is increased by approximately 25%, 13%, and 10% with Al$_2$O$_3$ (13 nm), Al$_2$O$_3$ (50 nm), and Fe$_3$O$_4$ (50 nm) NPs, respectively. As for the addition of SiO$_2$ NPs, it reduces the DC-BDV, whatever its concentration.

It is interesting to notice that the experimental results fit better to normal law (Table 4) instead Weibull distribution (Table 2). Indeed, hypothesis test of compliance of the average DC-BDV of investigated nanofluids complies totally with normal distribution while there is an exception as concerns the conformity with Weibull distribution that is SE/Fe$_3$O$_4$ at 0.2 g/L.

It should be noted that in the case of AC, the addition of the three investigated NPs increases the AC-BDV of the same SE; and that the highest AC-BDV was obtained using Fe$_3$O$_4$ conducting nanoparticles of size 50 nm at a concentration 0.4 g/L; the improvement was approximately 48% with respect to the SE alone [19]. As for SiO$_2$ (50 nm), the most
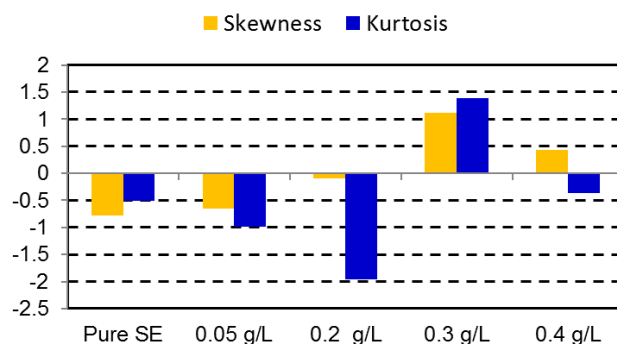

FIGURE 18. Histogram of DC SE/Fe$_3$O$_4$.

FIGURE 19. Skewness and kurtosis of DC SE/Fe$_3$O$_4$.

significant improvement in AC-BDV was approximately 32% for a concentration of 0.4 g/L. Furthermore, the highest AC-BDV using Al$_2$O$_3$ of size 13 nm and Al$_2$O$_3$ of size 50 nm, was 35% and 25% for 0.05 g/L and 0.3 g/L concentrations, respectively.

Note that with the two NP sizes of Al$_2$O$_3$ investigated (13 and 50 μm), the improvement in DC-BDV for basic

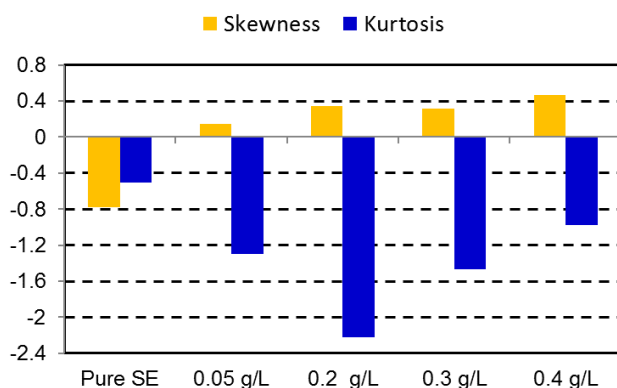insulating liquids is all the better as the nanoparticles are small, due to the large volume fraction of the nanoparticle interface - host liquid which results in a more significant accumulation of charge carriers (electrons) at these interfaces. Consequently, the number of free electrons taking part in the propagation of the streamers will be reduced thus slowing down the streamer and thereby increasing the breakdown voltage.

On the other hand, the theory which considers that the conducting NPs can trap and accumulate more electrons on their surfaces and thus slow down the propagation of streamers/discharges, thus increasing the breakdown voltage [29], [31], is debatable in the case of SEs under DC as evidenced by Al_2O_3 as opposed to Fe_3O_4.

According to Hwang *et al.* [29], when submitted to an electric field, the nanoparticles present in the fluid electrify by the injected charge carriers, mainly by electrons due to their very high mobility compared to that of ions. When the electrons deposited uniformly on the surfaces of nanoparticles, they create a local electric field which will oppose to the external electric field. The Charging dynamic of nanoparticles depends on their size and conductivity. The nanoparticles will act as ''electron (shallow) traps'' inside the nanofluid. They slow down the streamers propagation and thence increase the breakdown voltage. Such a theory has been advanced for conductive nanoparticles in the presence of lightning impulse voltage; it cannot be explain the phenomena observed with non-conducting nanoparticles under a DC stress as it is the case in this study.

By measuring the charge trap and transportation characteristics of pure transformer oil and transformer oil-TiO_2 based nanofluids submitted to AC and positive impulse voltage using thermally stimulated current method (TSC) and pulse electroacoustic technique (PEA), Du *et al.* [30] found that electron shallow and trap density and charge decay rate are greatly increased in nanofluids. They concluded that fast electrons may be converted to slow electrons by electron trapping and de-trapping in shallow traps of nanofluids, resulting in improved breakdown voltage compared to that of pure oil.

The increase in the DC-BDV in the case of Al_2O_3 and Fe_3O_4 NPs could be attributed to different mechanisms. These NPs can act by increasing the inception threshold voltage or by slowing down the propagation of streamers/discharges that increase breakdown voltage.

The nanoparticles act as sites for the accumulation of electrons on their surfaces until the interface is saturated, thus reducing the number of charge carriers directed toward the opposite electrode. Once the double layer is saturated, the electrons that are later encountered can no longer be trapped and participate in the development of streamers, thereby reducing the breakdown voltage. This can thus explain the concept of optimal concentration; it is the threshold beyond which electrons are no longer stopped. This process thus explains the concept of capture and release of electrons.

V. CONCLUSION

In this study, the DC dielectric withstand of MIDEL 7131 SE liquid mixed with conductive (Fe_3O_4) and insulating (Al_2O_3 and SiO_2) nanoparticles was investigated. The following results can be outlined:

- The optimal enhancement of the DC-BDV for a SE was obtained with the addition of Al_2O_3 (13 nm), where the improvement was approximately 25%, contrary to the AC-BDV of the SE where the most significant improvement of approximately 48% was obtained using Fe_3O_4 (50 nm).

- An optimum concentration of nanoparticles exists that aids in obtaining the greatest DC-BDV of the SE.

- The addition of SiO_2 NPs reduces the DC-BDV, regardless of its concentration.

- The DC-BDV values of the investigated NF samples comply with the normal distribution and, in most cases, with the Weibull distribution.

REFERENCES

[1] C. P. McShane, ''Natural and synthetic ester dielectric fluids: Their relative environmental, fire safety, and electrical performance,'' in *Proc. IEEE Ind. Commercial Power Syst. Tech. Conf.*, Sparks, NV, USA, May 1999, p. 8.

[2] H. Borsi and E. Gockenbach, ''Properties of ester liquid midel 7131 as an alternative liquid to mineral oil for transformers,'' in *Proc. IEEE Int. Conf. Dielectr. Liquids*, Coimbra, Portugal, Jun./Jul. 2005, pp. 377–380.

[3] *MIDEL Selection Guide*, M&I Mater. Limited, Manchester, U.K., Mar. 2017.

[4] L. Godson, B. Raja, D. M. Lal, and S. Wongwises, ''Enhancement of heat transfer using nanofluids—An overview,'' *Renew. Sustain. Energy Rev.*, vol. 14, pp. 629–641, Feb. 2010.

[5] Y. Xuan and Q. Li, ''Heat transfer enhancement of nanofluids,'' *Int. J. Heat Fluid Flow*, vol. 21, pp. 58–64, Feb. 2000.

[6] J. A. Eastman, S. U. S. Choi, S. Li, W. Yu, and L. J. Thompson, ''Anomalously increased effective thermal conductivities of ethylene glycol-based nanofluids containing copper nanoparticles,'' *Appl. Phys Lett.*, vol. 78, pp. 718–720, Feb. 2001.

[7] S. U. S. Choi, Z. G. Zhang, W. Yu, F. E. Lockwood, and E. A. Grulke, ''Anomalous thermal conductivity enhancement in nanotube suspensions,'' *Appl. Phys. Lett.*, vol. 79, pp. 2252–2254, Oct. 2001.

[8] G. Dombek, Z. Nadolny, and A. Marcinkowska, ''Effects of nanoparticles materials on heat transfer in electro-insulating liquids,'' *Appl. Sci.*, vol. 8, no. 12, p. 2538, Dec. 2018.

[9] D. A. Firlianda, A. A. Permanasari, P. Puspitasari, and S. Sukarni, ''Heat transfer enhancement using nanofluids (MnFe2O4-ethylene glycol) in mini heat exchanger shell and tube,'' *AIP Conf. Proc.*, vol. 2120, Jul. 2019, Art. no. 050014.

[10] P. Puspitasari, A. A. Permanasari, M. S. Shaharun, and D. I. Tsamroh, ''Heat transfer characteristics of NiO nanofluid in heat exchanger,'' *AIP Conf. Proc.*, vol. 2228, Apr. 2020, Art. no. 030023.

[11] V. Segal, A. Hjortsberg, A. Rabinovich, D. Nattrass, and K. Raj, ''AC (60 Hz) and impulse breakdown strength of a colloidal fluid based on transformer oil and magnetite nanoparticles,'' in *Proc. Conf. Rec. IEEE Int. Symp. Electr. Insul.*, Arlington, VA, USA, Jun. 1998, pp. 619–622.

[12] Y. Lv, Y. Zhou, C. Li, Q. Wang, and B. Qi, ''Recent progress in nanofluids based on transformer oil: Preparation and electrical insulation properties,'' *IEEE Elect. Insul. Mag.*, vol. 30, no. 5, pp. 23–32, Sep. 2014.

[13] R. Madavan and B. Sujatha, ''Investigation on effects of different types of nanoparticles on critical parameters of nano-liquid insulation systems,'' *J. Mol. Liquids*, vol. 230, pp. 437–444, Mar. 2017.

[14] J. Li, Z. Zhang, P. Zou, S. Grzybowski, and M. Zahn, ''Preparation of a vegetable oil-based nanofluid and investigation of its breakdown and dielectric properties,'' *IEEE Elect. Insul. Mag.*, vol. 28, no. 5, pp. 43–50, Sep. 2012.

[15] G. D. Peppas, V. P. Charalampakos, E. C. Pyrgioti, M. G. Danikas, A. Bakandritsos, and I. F. Gonos, ''Statistical investigation of AC breakdown voltage of nanofluids compared with mineral and natural ester oil,'' *IET Sci. Meas. Technol*, vol. 10, no. 6, pp. 644–652, 2016.

[16] M. Makmud, H. Illias, C. Chee, and M. Sarjadi, "Influence of conductive and semi-conductive nanoparticles on the dielectric response of natural ester-based nanofluid insulation," *Energies*, vol. 11, no. 2, p. 333, Feb. 2018.

[17] R. Madavan, S. S. Kumar, and M. W. Iruthyarajan, "A comparative investigation on effects of nanoparticles on characteristics of natural esters-based nanofluids," *Colloids Surf. A, Physicochemical Eng. Aspects*, vol. 556, pp. 30–36, Nov. 2018.

[18] U. Khaled and A. Beroual, "AC dielectric strength of synthetic ester-based Fe_3O_4, Al_2O_3 and SiO_2 nanofluids–conformity with normal and weibull distributions," *IEEE Trans. Dielectr. Electr. Insul.*, vol. 26, no. 6, pp. 625–633, Apr. 2019.

[19] U. Khaled and A. Beroual, "AC dielectric strength of mineral oil-based Fe_3O_4 and Al_2O_3 nanofluids," *Energies*, vol. 11, no. 12, p. 3505, Dec. 2018.

[20] H. B. H. Sitorus, R. Setiabudy, S. Bismo, and A. Beroual, "Jatropha curcas methyl ester oil obtaining as vegetable insulating oil," *IEEE Trans. Dielectr. Electr. Insul.*, vol. 23, no. 4, pp. 2021–2028, Aug. 2016.

[21] V.-H. Dang, A. Beroual, and C. Perrier, "Comparative study of statistical breakdown in mineral, synthetic and natural ester oils under AC voltage," in *Proc. IEEE Int. Conf. Dielectr. Liquids*, Trondheim, Norway, Jun. 2011, pp. 26–30.

[22] S. S. Shapiro and M. B. Wilk, "An analysis of variance test for normality (complete samples)," *Biometrika*, vol. 52, nos. 3–4, pp. 591–611, Dec. 1965.

[23] T. W. Anderson and D. A. Darling, "Asymptotic theory of certain 'Goodness of Fit' criteria based on stochastic processes," *Ann. Math. Statist.*, vol. 23, no. 2, pp. 193–212, Jun. 1952.

[24] W. Weibull, "A statistical distribution function of wide applicability," *J. Appl. Mech.*, vol. 18, no. 3, pp. 293–297, 1951.

[25] F. Palisson, "Détermination des paramètres du modèle de Weibull à partir de la méthode de l'actuariat," *Revue de Statistique Appliquée, tome*, vol. 37, no. 4, pp. 5–39, 1989.

[26] V. Dang, A. Beroual, and C. Perrier, "Comparative study of streamers in natural esters for high voltage applications and nutrition esters under lightning impulse voltage," *Int. Rev. Elect. Eng.*, vol. 6, no. 5, pp. 2675–2680, 2011.

[27] (Jul. 2, 2018). *The R Project for Statistical Computing Version 3.5.1*. [Online]. Available: https://www.r-project.org

[28] V.-H. Dang, A. Beroual, and C. Perrier, "Comparative study of statistical breakdown in mineral, synthetic and natural ester oils under AC voltage," *IEEE Trans. Dielectr. Electr. Insul.*, vol. 19, no. 5, pp. 1508–1513, Oct. 2012.

[29] J. G. Hwang, M. Zahn, F. M. O'Sullivan, L. A. A. Pettersson, O. Hjortstam, and R. Liu, "Effects of nanoparticle charging on streamer development in transformer oil-based nanofluids," *J. Appl. Phys.*, vol. 107, no. 1, Jan. 2010, Art. no. 014310.

[30] Y. Du, Y. Lv, C. Li, M. Chen, J. Zhou, X. Li, Y. Zhou, and Y. Tu, "Effect of electron shallow trap on breakdown performance of transformer oil-based nanofluids," *J. Appl. Phys.*, vol. 110, no. 10, Nov. 2011, Art. no. 104104.

[31] J. Miao, M. Dong, M. Ren, X. Wu, L. Shen, and H. Wang, "Effect of nanoparticle polarization on relative permittivity of transformer oil-based nanofluids," *J. Appl. Phys.*, vol. 113, no. 20, May 2013, Art. no. 204103.

ABDERRAHMANE BEROUAL (Fellow, IEEE) was responsible for the Master's Research Program in electrical engineering, from 2013 to 2015. He supervised more than 45 Ph.D. degree theses. He is currently a Distinguished Professor with the Ecole Centrale de Lyon, University of Lyon, France. He is also the Head of the High Voltage Group at AMPERE Lab, CNRS, and a Scientific Expert with the SuperGrid Institute. He is a member of many advisory committees of international conferences, the Technical Committee of the IEEE CEIDP, and the UF10 Technical Commission-MT30 of the IEC. He has authored or coauthored more than 480 technical articles, including more than 210 refereed journal articles, two books, and six book chapters. He holds five patents. His main research interests include high-voltage insulation, outdoor insulation, dielectric materials, long air gaps discharge and lightning, and the modeling of discharges and composite materials. He is a Distinguished Visiting Professor of the U.K. Royal Academy of Engineering with Cardiff University and King Saud University, Saudi Arabia. He was the recipient of the IEEE T. Dakin Award, in 2016. From 1994 to 1998, he chaired the International Study Group on Streamer Propagation in Liquids of the IEEE DEIS. He is an Associate Editor of the IEEE Transactions on Dielectrics and Electrical Insulation.

USAMA KHALED received the bachelor's and M.Sc. degrees in electrical engineering from Aswan University, Egypt, in 1998 and 2003, respectively, and the Ph.D. degree in electrical engineering from Cairo University, Egypt, and Kyushu University, Japan, through a joint scholarship, in 2010. Since 2000, he has been with the Department of Electrical Power Engineering, Faculty of Energy Engineering, Aswan University, working as a Teaching Assistant, an Assistant Lecturer, an Assistant Professor, and an Associate Professor. He has been working as an Assistant Professor and an Associate Professor with the College of Engineering, King Saud University, since 2014 and 2018, respectively. His research interests include nano-dielectric materials, applied electrostatics, and high-voltage technologies.

AASSEM M. ALGHAMDI received the B.S. degree (Hons.) in electrical engineering from Al-Baha University, Al-Baha, Saudi Arabia, in 2014, and the master's degree in electrical engineering from King Saud University, in 2020. He has been working as a Transmission Engineer with the Maintenance Department, Saudi Electricity Company, Riyadh, since 2014.

• • •